



HOTAIR Induces Methylation of PCDH10, a Tumor Suppressor Gene, by Regulating DNMT1 and Sponging with miR-148b in Gastric Adenocarcinoma

Seung In Seo^{1,2*}, Jung-Ho Yoon^{3*}, Hyo Joo Byun^{3,4}, and Sang Kil Lee^{3,4}

¹Department of Internal Medicine, Kangdong Sacred Heart Hospital, Hallym University College of Medicine, Seoul;

²Department of Medicine, The Graduate School, Yonsei University, Seoul;

³Division of Gastroenterology, Department of Internal Medicine, Institute of Gastroenterology, Yonsei University College of Medicine, Severance Hospital, Seoul;

⁴Brain Korea 21 PLUS Project for Medical Science, Yonsei University, Seoul, Korea.

Purpose: HOX transcript antisense intergenic RNA (HOTAIR), as a long non-coding RNA, has been reported to regulate carcinogenesis by epigenetic mechanism in various cancers. Protocadherin 10 (PCDH10) is one of the well-known tumor suppressor genes, and is frequently methylated in gastric cancers (GC). We aimed to investigate the detailed pathway of how HOTAIR contributes to the target gene in gastric carcinogenesis.

Materials and Methods: We investigated the mechanism of HOTAIR on carcinogenesis and metastasis of GC. Methylation-specific PCR was performed to identify the interaction between HOTAIR and PCDH10. In addition, we investigated the interaction between miR-148b and HOTAIR by dual-luciferase reporter assay and RNA immunoprecipitation (RIP) assay.

Results: The expression of HOTAIR was significantly upregulated in GC tissues ($p < 0.05$) and GC cell lines ($p < 0.01$), while PCDH10 was downregulated in GC tissues ($p < 0.05$). The knockdown of HOTAIR (si-HOTAIR1 and 2) significantly upregulated the mRNA/protein expression of PCDH10 and reduced the methylation of PCDH10 compared to the control in MKN 28 and MKN 74. Si-HOTAIR1 and 2 significantly reduced DNA methyltransferase 1 (DNMT1) expression, and overexpression of HOTAIR increased DNMT1 expression. In RIP, we found that miR-148b interacted with HOTAIR. Si-HOTAIRs increased miR-148b expression, and miR-148b mimic inversely reduced HOTAIR expression. Si-HOTAIRs and miR-148b mimic reduced DNMT1 expression and increased PCDH10 expression compared to the control.

Conclusion: This study demonstrated that HOTAIR interacts with miR-148b and DNMT1, eventually leading to PCDH10 methylation, which contributes to the progression of GC. Our findings provide a better understanding for detailed pathway of HOTAIR in epigenetic mechanism of GC.

Key Words: HOX transcript antisense intergenic RNA (HOTAIR), protocadherin 10, microRNA 148b, gastric cancer, methylation

Received: October 28, 2020 **Revised:** November 18, 2020

Accepted: December 7, 2020

Corresponding author: Sang Kil Lee, MD, PhD, Division of Gastroenterology, Department of Internal Medicine, Institute of Gastroenterology, Yonsei University College of Medicine, 50-1 Yonsei-ro, Seodaemun-gu, Seoul 03722, Korea.
Tel: 82-2-2224-2771, Fax: 82-2-478-6925, E-mail: sklee@yuhs.ac

*Seung In Seo and Jung-Ho Yoon contributed equally to this work.

•The authors have no potential conflicts of interest to disclose.

© Copyright: Yonsei University College of Medicine 2021

This is an Open Access article distributed under the terms of the Creative Commons Attribution Non-Commercial License (<https://creativecommons.org/licenses/by-nc/4.0>) which permits unrestricted non-commercial use, distribution, and reproduction in any medium, provided the original work is properly cited.

INTRODUCTION

Although the incidence of gastric cancer (GC) has declined worldwide, it remains the sixth leading cancer and third most common cause of cancer deaths around the globe.^{1,2} The incidence of GC is disproportionately high in East Asia. Overall, declining *Helicobacter pylori* (*H. pylori*) prevalence has resulted in reduced GC incidence and mortality; however, the detailed mechanism of gastric carcinogenesis is still unclear.

Recent studies have demonstrated that long non-coding RNAs (lncRNAs) are associated with chromatin remodeling

complexes and lncRNAs act by guiding epigenetic regulators to specific loci to alter DNA methylation or histone status.^{3,4} lncRNA is also known to function as a competitive endogenous RNA (ceRNA) by sponging target miRNAs.⁵ Over the last decade, remarkable progresses about GC-associated lncRNAs have been achieved.⁵ HOX transcript antisense intergenic RNA (HOTAIR) is one of the well-known lncRNAs that regulate gene expression by mediating the modulation of chromatin structure.⁶⁻¹⁴

Previous genome-wide and microarray studies showed specific target genes following HOTAIR overexpression.⁷ In breast cancer, protocadherin 10 (PCDH10) was transcriptionally repressed upon HOTAIR expression.⁷ PCDH10 is known to be a member of the protocadherin gene family, which is a direct p53 transcriptional target and acts as an important tumor suppressor gene by regulating tumor cell motility and migration in multiple cancers, including GC.¹⁵⁻¹⁷ Furthermore, in our previous study of gastrointestinal stromal tumor (GIST), microarray showed that TP53 was downregulated mostly after HOTAIR overexpression.¹⁸ Based on this finding, it is possible to infer that a regulatory mechanism may exist among HOTAIR, PCDH10, and p53.

To date, some studies have documented the important prognostic role of lncRNA HOTAIR on GC. However, studies on how HOTAIR contributes to the target genes in gastric carcinogenesis, in combination with miRNA, are still rare. In addition, the association between HOTAIR and PCDH10 has not yet been reported in GC. Therefore, this study aimed to investigate the mechanistic role of HOTAIR and PCDH10 in GC.

MATERIALS AND METHODS

Patients and tissue samples

Forty-nine GC tissue and paired adjacent gastric tissue samples were collected from 49 patients who underwent surgical resection or endoscopic resection for GC at Kangdong Sacred Heart Hospital, Hallym University College of Medicine. All samples were frozen in liquid nitrogen immediately after resection and stored at -80°C until use. The mean age of patients was 62.2±1.7 years, and the male/female ratio was 65.3%. This study was approved by the Ethics Committee of Kangdong Sacred Heart Hospital, and written informed consent was obtained from all patients (IRB no. 2017-11-007).

Cell lines and cell culture

A total of five GC cell lines (Kato III, MKN 28, MKN 45, MKN 74, AGS) and normal GES-1 cell line were used. Human GC cells were cultured in RPMI-1640 medium (Thermo Scientific, Rockford, IL, USA) supplemented with 10% fetal bovine serum (FBS), 1% penicillin, and streptomycin. The GC cells were incubated at an atmosphere of 5% CO₂ and 95% air at 37°C.

RNA extraction, reverse transcription, and quantitative real-time PCR

Total RNA was extracted from 49 GC tissues and cell lines using TRIzol reagent (Invitrogen, Carlsbad, CA, USA). For cDNA synthesis, 2.0 µg of total RNA was reverse transcribed according to the manufacturer's protocol. The level of HOTAIR was measured by real-time PCR using iQ SYBR Green Supermix (Applied Biosystems Inc., Carlsbad, CA, USA). Ct value of the sample was normalized to the U6 or GAPDH expression, and the 2^{-ΔΔCt} method was used to calculate the relative level. The primers used for this study are listed in Table 1.

Small interfering RNA transfection

MKN 28 and MKN 74 cells (2×10⁵) were plated in 6-well culture plates and transfected after incubation for 24 h. Small interfering RNA (siRNA) and nonspecific control siRNA were synthesized (Invitrogen), and cells were transfected using Lipofectamine 2000 (Invitrogen). Target sequences for HOTAIR siRNAs were designed as follows: si-HOTAIR1, Sense: 50-GAACGGGAGUACAGAGAGAUU-30, Antisense: 50-AAUCUCUCUGUACUCCCGUUC-30; si-HOTAIR2, Sense: 50-CA CAUGAACGCCAGAGAUU-30, Antisense: 50-AAUCUCU GGGCGUUCAUGUGG-30.

HOTAIR-overexpressing plasmid construction

To overexpress HOTAIR in AGS cell, we used human HOTAIR cDNA (Addgene, Plasmid #26110, Cambridge, MA, USA).¹⁸ The HOTAIR cDNA was amplified using a PCR system, and the resulting product was inserted in the pcDNA3.1 vector (Addgene,

Table 1. Primer Sequences Used for qRT-PCR

Primer name	Direction	Sequences (5' to 3')
HOTAIR	Forward	TGGGAGTGTGTTTTGTTGGA
	Reverse	CTACACAACCCCTTCGCTTC
PCDH10	Forward	AACGGTGGAGATGAGGACAG
	Reverse	TCTCCGGATGGATGTTCTTC
DNMT1	Forward	GCCTCTCTCCGTTTGGTACA
	Reverse	TCGGAGGCTTCAGCAGAC
EZH2	Forward	CCTCGAGTACTGTGGGCAAT
	Reverse	CACCTTGCAGCTGGTGAGAA
SUZ12	Forward	AGTTACTCGGCCTCCTCCTC
	Reverse	AGGAAAAGCTCGTGGTCAGC
p53	Forward	CACATGACGGAGGTTGTGAG
	Reverse	ACACGCAAATTTCTTCCAC
U6	Forward	CTCGCTTCGGCAGCACA
	Reverse	AACGCTTCAGGAATTTGCGT
GAPDH	Forward	CCGGGAAACTGTGGCGTGATGG
	Reverse	AGGTGGAGGAGTGGGTGTCGCTGTT
miR-148b		UCAGUGCAUCACAGAACUUUGU

HOTAIR, HOX transcript antisense intergenic RNA; PCDH10, protocadherin 10; DNMT1, DNA-methyltransferase 1; EZH2, enhancer of zeste 2; SUZ12, suppressor of zeste 12; GAPDH, glyceraldehyde 3-phosphate dehydrogenase; miR-148b, microRNA-148b

Plasmid #47388) using TOPO cloning (Invitrogen) according to the manufacturer's protocol. The HOTAIR-expressing vector was sequenced and analyzed using Macrogen (Macrogeninc., Seoul, Korea). AGS cell was transfected with 1 µg pcDNA3.1-HOTAIR (pcDNA-HOTAIR) for 24 h using Lipofectamine 2000 (Invitrogen).

Cell proliferation analysis

MKN 28 and MKN 74 cells were transfected with 50 nM of si-HOTAIRs, and AGS cell was transfected with pcDNA-HOTAIR from 0 to 72 h. MTS assays (Promega, Madison, WI, USA) were used to measure cell proliferation in 96-well plates. The number of viable cells was determined by reaction with MTS reagent for 1 h in the dark, and the products of the reaction were measured by enzyme-linked immunosorbent assay (ELISA). Luminescence activity was measured using a Luminescence Microplate Reader (Molecular Devices Co., Sunnyvale, CA, USA).

Apoptosis analysis

MKN 28 and MKN 74 cells were transfected with si-HOTAIRs or si-Control (siCT), and washed with 1X phosphate buffered saline (PBS; Thermo Scientific). After 48 h, the cells were pelleted and washed with PBS. After washing with 1X binding buffer (BD Bioscience, San Jose, CA, USA), the cells were stained with fluorescein isothiocyanate (FITC)-Annexin V and PI, using a FITC-Annexin V kit (BD Bioscience). The apoptotic ratio was measured using flow cytometry (BD Bioscience), and caspase 3/7 protein levels were calculated by ELISA after treatment with si-HOTAIRs.

Cell cycle analysis

MKN 28 and MKN 74 cells were transfected with 100 nM of si-HOTAIRs or siCT, washed with PBS, and then fixed with 75% ethanol overnight at -20°C. Cells were resuspended in PBS and treated with RNase for 30 min at room temperature. The cell nucleus was stained with propidium iodide (Sigma, Saint Louis, MO, USA), and incubated for 20 min in the dark. The proportion of cells within cell cycle phases were determined by flow cytometry (BD Biosciences), and analyzed with FlowJo7.6 program (Treestar, Ashland, OR, USA).

Invasion assay and migration assay

To perform invasion assay, the matrigel invasion assay was performed using BD biocoat trans-wells (BD Biosciences). MKN 28 and MKN 74 cells were transfected with si-HOTAIRs or si-CT. After 48 h, the transfected cells were re-plated in the upper chamber containing RPMI-1640 medium. The lower chamber was filled with RPMI-1640 medium containing 10% FBS. After 48 h, non-invading cells within the insert chamber were removed, and the upper layer of the trans-well was wiped with a cotton swab. The membrane of the bottom part of the upper chamber was fixed and stained with Diff-Quik solution

(Dade Behring Inc., Newark, DE, USA). Invading cells were visualized using a virtual microscope (BX51; Olympus, Tokyo, Japan) in five random fields, counted, and averaged.

For migration analysis, GC cells were transfected with si-HOTAIRs and si-CT. The cells were grown for 48 h, and a wound was then generated using a P-20 tip. The width of scratched cells was measured at 0 and 48 h under a virtual microscope (BX51).

Western blot

The cells were lysed in 1_ RIPA buffer (Cell Signaling Technology, Danvers, MA, USA) containing protease inhibitor. Extracted proteins were separated by 8% to 10% SDS-polyacrylamide gel electrophoresis and transferred to a polyvinylidene difluoride membrane (GE Healthcare, Piscataway, NJ, USA). The membrane was blocked for 1 h at room temperature in tris-phosphate buffer containing 0.1% tween 20 with 5% skim-milk (BD Biosciences), and subsequently incubated at room temperature for 1-2 h with primary antibodies. The following primary antibodies were used for Western blot analysis:

PARP (Cell Signaling Technology, #9542), bcl-2 (Cell Signaling Technology, #2870), bcl-xl (Cell Signaling Technology, #2764), p53 (Santa Cruz Biotechnology, Santa Cruz, CA, USA, sc-126), cleaved caspase-9 (Cell Signaling Technology; 9504), SUZ12 (Abcam, Cambridge, MA, USA, ab12073), PCDH10 (Thermo Scientific, Cell Signaling Technology, #7237, PA5-31042), Vimentin (1:2000, Santa Cruz Biotechnology, sc-373717), Snail (1:1000, Cell Signaling Technology, 3879s), Slug (1:1000, Santa Cruz Biotechnology, sc-166476), Src (1:1000, Santa Cruz Biotechnology, sc-8056), β-actin (Bioworld Technology, Louis Park, MN, USA, AP0060), EZH2 (Abcam, ab186006), and DNMT1 (Abcam, ab13537).

Methylation-specific PCR

Genomic DNA was extracted from MKN 28 and MKN 74 cells using a DNeasy Blood & Tissue kit (Qiagen, Valencia, CA, USA). An EZ DNA methylation-gold kit (ZymoResearch, Irvine, CA, USA) was used for DNA bisulfate transformation. The following methylation-specific PCR (MS-PCR) primers for PCDH10 were used as described: methylation (forward: GTTAGGGAG GATGGATGTAAGTATC, reverse: GCG AAATAAAAACAATA AAACGAC), and un-methylation (forward: GTTAGGGAGGA TGGATGTAAGTATT, reverse: CCCACA AAATAA AAACAATAA AA AA).

RNA immunoprecipitation

For immunoprecipitation of endogenous RNA-protein complexes, cells were lysed with IP buffer (Thermo Fisher Scientific, Waltham, MD, USA), and resuspended in RNA immunoprecipitation (RIP) buffer (Abcam) with RNase inhibitor (GenDEPOT) and protease inhibitor (GenDEPOT, Barker, TX, USA). For shearing of chromatin, we used 20 cycles of shearing under cooling conditions, with 15 s on and 30 s off for each cy-

cle (170–190 W) and water bath sonication. After sonication, the antibodies were added to the supernatant obtained by centrifugation, and then incubated overnight at 4°C with a rotator. After incubation, 20 µL of MagnaChip protein magnetic beads (Millipore, Darmstadt, Germany) were added, and samples were reacted on a rotator at 4°C for 1 h. After washing twice with RIP buffer, samples were dissolved with TRIzol reagent or RIPA.

Luciferase reporter assay

For the luciferase reporter assay, GC cells were co-transfected

with miRNAs (miR-148b mimics or miR-148b inhibitors; Biomics Biotechnologies Co., Ltd., Nantong, China) and reporter vectors (pmirGLOWT or pmirGLOMUT) using Lipofectamine 2000. Luciferase activity was assayed 48 h after transfection using a DualLuciferase Reporter Assay system (Beyotime Institute of Biotechnology, Haimen, China). The values were normalized to those obtained for miRNA negative control transfection. All transfection experiments were performed in triplicate.

Statistical analysis

All of the analyzed data for continuous and categorical vari-

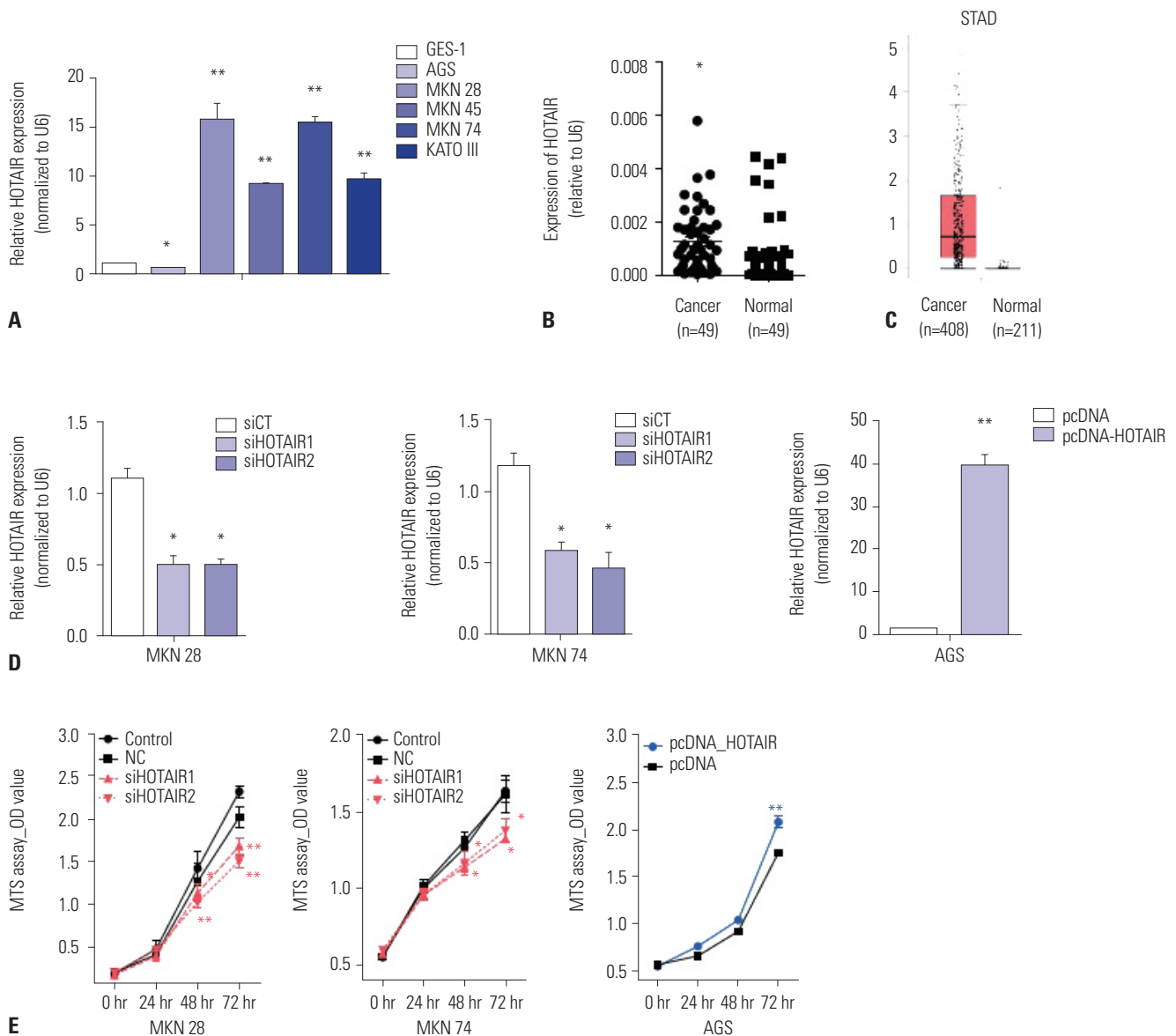


Fig. 1. HOTAIR was overexpressed in GC cell lines and tissues, and knockdown of HOTAIR repressed GC cell proliferation. (A) The relative expression of HOTAIR by qRT-PCR in five GC cell lines. (B) The relative expression of HOTAIR by qRT-PCR in 49 GC tissues and paired non-tumor tissues. (C) The relative expression of HOTAIR in GC tissues and adjacent gastric tissues by TCGA data. (D) MKN 28 and MKN 74 cells were transfected with siHOTAIR1, siHOTAIR2, and/or scrambled RNA; and AGS cell was transfected with pcDNA and pcDNA-HOTAIR. The relative HOTAIR expression by qRT-PCR assay is shown. (E) Cell viability was detected by MTS assay. Data are presented as the mean \pm standard deviation of three independent experiments. The asterisk (*) represents a statistically significant difference compared with scrambled control. * $p \leq 0.05$, ** $p \leq 0.01$. HOTAIR, HOX transcript antisense intergenic RNA; GC, gastric cancer; TCGA, The Cancer Genome Atlas.

ables are presented as the mean±standard error and the number of lesions with the percentage. Statistical tests used to compare the measured results included the t-test, chi-square test, and Fisher's exact test. The expressions of HOTAIR in GC were categorized into low and high groups based on the median value of HOTAIR expression in GC tissue. A *p*-value<0.05 indicated a statistically significant difference for comparisons between groups. All of the statistical procedures were conducted using the statistical software SPSS for Windows (version 18.0; SPSS Inc., Chicago, IL, USA).

RESULTS

HOTAIR expression in GC cell lines and GC tissues

The relative RNA level of HOTAIR was higher in MKN 74, MKN 28, MKN 45, and KATO III cells compared to normal gastric cell line GES-1 (*p*<0.01); however, the level of HOTAIR in AGS cell was lower than that in GES-1 (*p*<0.05) (Fig. 1A). The expression of HOTAIR in GC tissues were significantly higher than

that in non-tumor tissue (*p*<0.05) (Fig. 1B). The Cancer Genome Atlas data showed similar result (Fig. 1C). After transfection with si-HOTAIR, HOTAIR was significantly downregulated in MKN 28 and MKN 74 cells (Fig. 1D, left panel). In AGS cell, which showed low expression of HOTAIR compared to other cancer cell lines, HOTAIR was overexpressed by transfection with pc-DNA-HOTAIR (Fig. 1D, right panel).

The effect of HOTAIR on proliferation and apoptosis of GC cells

We have already demonstrated that HOTAIR inhibits GC proliferation and apoptosis in the previous study¹⁴; however, in order to identify the reproducibility in a new experimental environment, we examined MTS assay. From 48 hr after treatment with si-HOTAIR1 and si-HOTAIR2, the proliferation of MKN 28 and MKN 74 were significantly reduced, respectively, compared to the si-CT (Fig. 1E). In the contrary, overexpression of HOTAIR upregulated the proliferation in AGS cell (Fig. 1E).

Next, we analyzed the effect of HOTAIR on apoptosis of MKN 28 and MKN 74 cells using PI/Annexin-V. Si-HOTAIRs were sig-

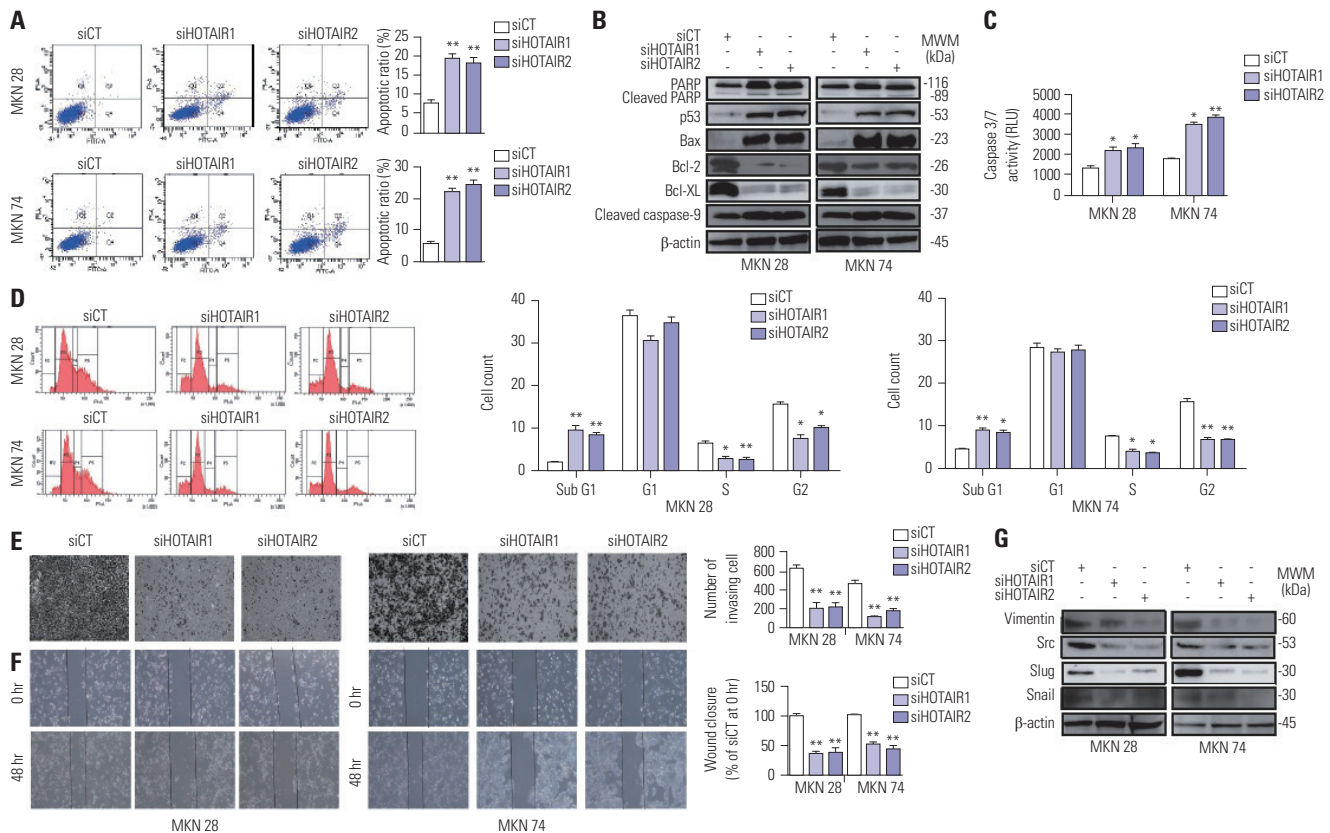


Fig. 2. Knockdown of HOTAIR induced cell apoptosis and inhibited invasiveness and migratory capacity. (A) PI/annexin-V staining on flow cytometry was performed in transfected MKN 28 and MKN 74 cells (A; left panel), and the apoptotic ratio was measured by flow cytometry (A; right panel). (B) Western blot analysis of apoptotic markers after treatment with si-HOTAIRs. (C) Caspase Glo 3 and 7 assays after treatment with si-HOTAIRs. (D) Cell cycle distributions was analyzed by flow cytometry in GC. (E) Matrigel invasion assay after transfection with si-HOTAIRs. (F) Wound healing assay after transfection with si-HOTAIRs. The width of the scratch wound was observed by microscopy at 0 and 48 h. (G) Western blot analysis of epithelial-mesenchymal transition markers after treatment with si-HOTAIRs. The asterisk (*) represents a statistically significant difference compared with scrambled control. **p*≤0.05, ***p*≤0.01. Data are presented as the mean±standard deviation of three independent experiments. HOTAIR, HOX transcript antisense intergenic RNA; GC, gastric cancer.

nificantly increased in the early-to-late apoptotic ratio compared to the control in both cell lines (Fig. 2A). Protein levels of two anti-apoptotic markers, such as Bcl-2 and Bcl-xL, were decreased by si-HOTAIRs, while an induction of apoptotic factors such as p53, Bax, cleaved caspase-9 and cleaved PARP were increased compared to the control cells (Fig. 2B). Si-HOTAIRs significantly increased the caspase 3/7 activity in MKN 28 and 74 cells (Fig. 2C). Flow cytometry analysis revealed a significant increase in the proportion of cells in the sub-G1 phase in si-HOTAIRs compared to siCT (Fig. 2D). Si-HOTAIRs subsequently reduced the proportion of cells in S and G2 compared to siCT (Fig. 2D). These data suggested that HOTAIR consistently inhibits apoptosis in GC cells.

The impact of HOTAIR on invasion and migration of GC cells

We have already shown that HOTAIR promotes the invasion and migration of GC cells¹⁴; however, in order to identify the reproducibility in a new experimental environment, we measured the migration and invasion of GC cells. We found that the knockdown of HOTAIR markedly inhibited cell invasive ability (Fig. 2E). Next, the effects of HOTAIR silencing on migratory capacity was confirmed by scratch wound healing assay. Compared to si-CT, wound closure was repressed by si-HOTAIRs (Fig. 2F). We measured the epithelial mesenchymal transition related proteins after the treatment of si-HOTAIR. When compared with siCT, si-HOTAIR down regulated Vimentin, Src, Slug, and Snail (Fig. 2G). This result showed that knockdown of HOTAIR suppressed GC cell migration.

The relation between HOTAIR expression and clinicopathologic characteristics of GC

Clinicopathologic features of GC were analyzed according to the median level of HOTAIR in GC tissues (Table 2). Diffuse and mixed type cancers by Lauren classification were more prevalent in the high HOTAIR group (high vs. low; diffuse and mixed type, 64.7% vs. 37.5%, $p=0.04$). Moreover, tumors in the high HOTAIR group showed a more advanced Tumor-Node-Metastasis (TNM) stage than those in the low HOTAIR group (high vs. low; stage II, III, 82.4% vs. 56.3%, $p=0.04$). The depth of tumor invasion showed more advanced T stage in the high HOTAIR group. Age, sex, proportion of *H. pylori* infection, carcinoembryonic antigen level, and histologic differentiation were not related to HOTAIR expression. In addition, lymphovascular invasion and lymph node metastasis were not statistically different according to the HOTAIR level.

The effect of HOTAIR on tumor suppressor gene, PCDH10, in GC

We noticed that HOTAIR knockdown reduced PCDH10 in breast cancer cell in microarray⁷; therefore, we need to validate PCDH10 as a new target of HOTAIR in GC. We performed qRT-PCR to analyze the mRNA level of PCDH10 in 49 GC tis-

Table 2. Clinicopathological Analysis according to Median Level of HOTAIR in Gastric Cancer

	High HOTAIR (n=17)	Low HOTAIR (n=32)	p value
Age	62.1±13.5	62.1±11.5	0.99
Sex, male (%)	12 (70.6)	20 (62.5)	0.75
<i>H. pylori</i>	8/17	16/32	0.30
CEA	3.2±3.2	2.5±2.5	0.50
PCDH10	0.0014±0.0016	0.01±0.012	<0.01
Lauren's classification			0.04
Intestinal	6 (35.3)	20 (62.5)	
Diffuse, mixed	11 (64.7)	12 (37.5)	
Differentiation			0.54
WD, MD	6 (35.3)	15 (46.9)	
PD, signet ring cell	11 (64.7)	17 (53.1)	
Lymphovascular invasion	12 (70.6)	21 (65.6)	0.49
Depth of tumor invasion			0.03
T1/T2	4 (23.5)	18 (56.3)	
T3/T4	13 (76.5)	14 (43.8)	
Lymph node metastasis	13 (76.5)	20 (62.5)	0.36
TNM stage			0.04
I	3 (17.6)	14 (43.8)	
II, III	14 (82.4)	18 (56.3)	

H. pylori, Helicobacter pylori; CEA, carcinoembryonic antigen; WD, well-differentiated; MD, moderately differentiated; PD, poorly differentiated. HOTAIR, HOX transcript antisense intergenic RNA; PCDH10, protocadherin 10; TNM, Tumor-Node-Metastasis.

Data are presented as mean±SD.

issues, and the mRNA of PCDH10 was significantly higher in adjacent non-tumor tissue compared to GC tissues ($p<0.05$) (Fig. 3A). We evaluated the protein level of PCDH10 by Western blot in four GC tissues. The expression of PCDH10 was downregulated in GC tissue; and oppositely, the expression of HOTAIR was upregulated in GC tissue (Fig. 3B).

We investigated the PCDH10 level in GC cells after knockdown of HOTAIR. Both si-HOTAIR1 and 2 significantly upregulated the mRNA of PCDH10 (Fig. 3C) and protein (Fig. 3D, upper panel) in MKN 28 and MKN 74. In MS-PCR, si-HOTAIR1 and 2 significantly reduced the methylation of PCDH10 compared to the control in MKN 28 and MKN 74 (Fig. 3D, lower panel). To investigate the related pathway of HOTAIR to control methylation of PCDH10, we performed RIP to identify the interaction between DNMT1, EZH2, SUZ12, and HOTAIR. HOTAIR significantly interacted with DNMT1 and EZH2, but not with SUZ12 (Fig. 3E). DNMT1 and EZH2 were downregulated by si-HOTAIRs in MKN 28 and MKN 74 cells, while overexpression of HOTAIR induced upregulation of DNMT1 and EZH2 in AGS cell (Fig. 3F).

Since PCDH10 is known as a transcriptional target of p53,¹⁵ we investigated the expression of PCDH10 and p53 after overexpression of HOTAIR. The overexpression of HOTAIR significantly reduced the translation and transcription of p53 in nor-

mal gastric cell line GES-1 (Fig. 3G and H). This result suggested that p53 reduction by HOTAIR may be a major cause of PCDH10 transcription reduction. Next, we conducted an experiment to compare the effects of p53 and HOTAIR on PCDH10 transcrip-

tion. In AGS cell, p53 significantly increased PCDH10 transcription; however, co-infection of HOTAIR, which is expected to induce the promoter methylation of PCDH10 and reduce PCDH10 transcription, reduced only a part of PCDH10 transcription by

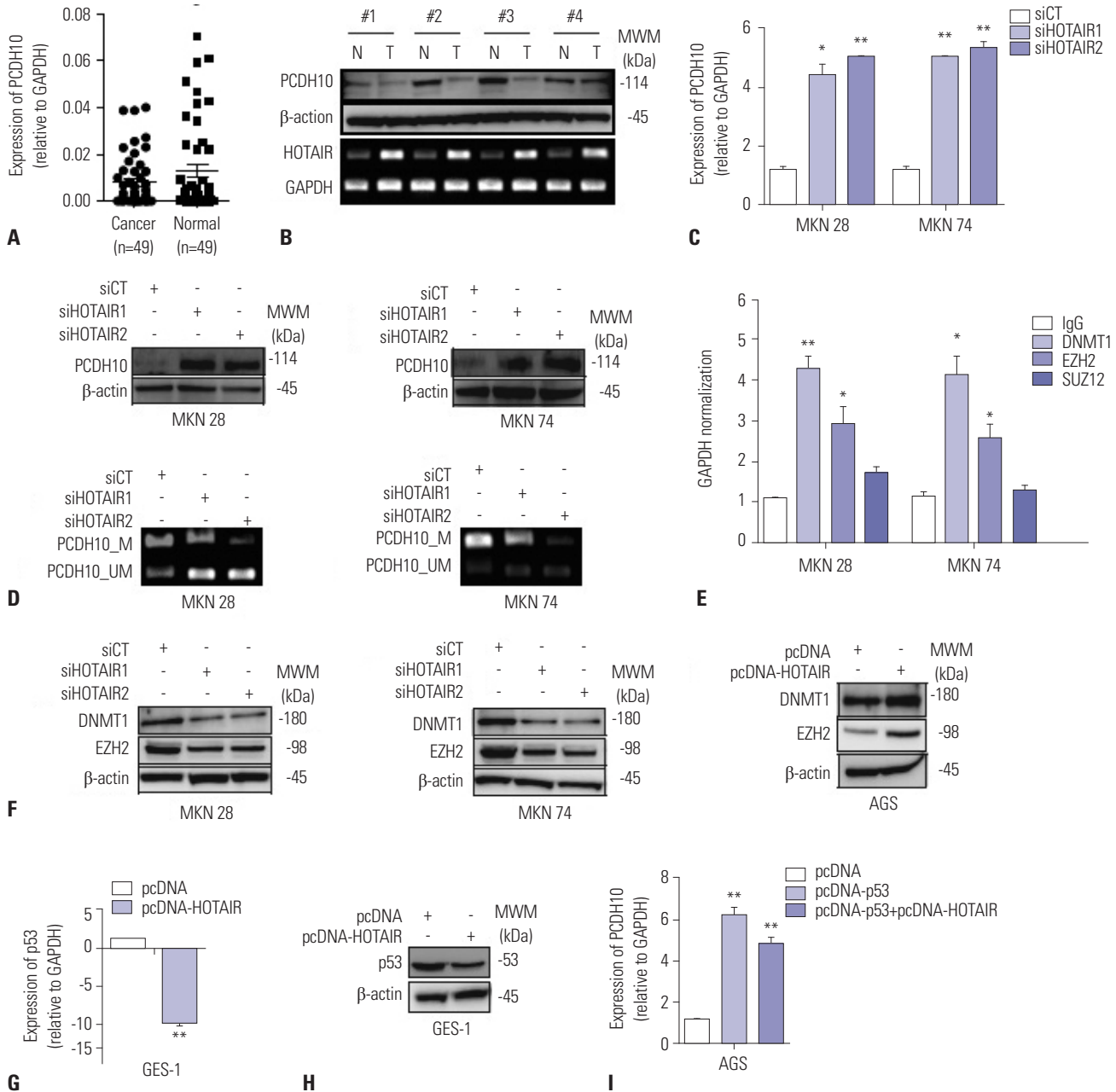


Fig. 3. HOTAIR promoted the methylation of PCDH10 by regulating EZH2 and DNMT1. (A) The relative expression of PCDH10 by qRT-PCR in GC tissues and paired adjacent gastric tissues. (B) Western blot analysis of PCDH10 and RT-PCR analysis of HOTAIR in four GC tissues and paired adjacent gastric tissues. (C) The relative expression of PCDH10 by qRT-PCR after transfection with si-HOTAIRs in MKN 28 and MKN 74 cells. (D) Western blot analysis of PCDH10 after treatment with si-HOTAIRs (upper panel), and MS-PCR analysis of PCDH10 after treatment with si-HOTAIRs. (E) The interaction between DNMT1, EZH2, and HOTAIR was confirmed by RIP analysis. The bars present relative enrichment. (F) Western blot analysis of DNMT1 and EZH2 after treatment with si-HOTAIRs in MKN 28 and MKN 74 cell lines and pcDNA-HOTAIR in AGS cell line. (G) The relative expression of p53 after transfection with pcDNA-HOTAIR in GES-1 cell by qRT-PCR. (H) Western blot analysis of p53 after transfection with pcDNA-HOTAIR in GES-1 cell. (I) The relative expression of PCDH10 after transfection with pcDNA-p53 and pcDNA-HOTAIR in AGS cell by qRT-PCR. Data are presented as the mean±standard deviation of three independent experiments. The asterisk (*) represents a statistically significant difference compared with scrambled control. * $p \leq 0.05$, ** $p \leq 0.01$. HOTAIR, HOX transcript antisense intergenic RNA; PCDH10, protocadherin 10; GC, gastric cancer; MS-PCR, methylation-specific PCR; RIP, RNA immunoprecipitation.

p53 (Fig. 3I). This result disproved the fact that although HOTAIR is involved in the transcription of PCDH10, the effect of p53 is greater than HOTAIR.

HOTAIR regulates methylation of PCDH10 as a ceRNA by sponging miR-148b

In a previous study, several potential miRNA targets of HOTAIR were identified in GC by computer-aided algorithm.¹⁹⁻²² In this study, we further explored the underlying mechanism of HOTAIR as ceRNA, and we examined miR-148b as target of HOTAIR, as it was down-regulated in GC in previous study.²⁰

The expression level of miR-148b was significantly lower in four GC cells, including MKN 28 and MKN 74, compared to GES-1 cell (Fig. 4A). In RIP, miR-148b interacted with HOTAIR in both MKN 28 and MKN 74 cells (Fig. 4B). Both si-HOTAIR1 and 2 increased the miR-148b expression (Fig. 4C), and the treatment of miR-148b mimic reduced the HOTAIR expression (Fig. 4D), indicating an inverse correlation between HOTAIR and miR-148b in GC cells.

To verify whether miR-148b regulates HOTAIR as a direct target, a predicted binding site for miR-148b was identified using an online software program,²³ and wild-type or mutant miR-148b target binding sequences were cloned into the pmirGLO luciferase vector. Following co-transfection with pmirGLO luciferase construct (pmirGLO-mutant or pmirGLO-wild-type) and miR-148b mimic or inhibitor, a dual luciferase assay was performed to determine the luciferase activity.

Our data showed that MKN 28 cell co-transfected with the constructs containing pmirGLO-Mut and miR-148b mimic had significantly higher luciferase activity compared to those transfected with pmirGLO-WT and miR-148b mimic ($p < 0.05$) (Fig. 4E). In MKN 74 cell, the result was similar with MKN 28. In addition, the relative luciferase activity was significantly lower in MKN 28 and MKN 74 cells co-transfected with the constructs containing pmirGLO-Mut and inhibitor of miR-148b compared to those transfected with pmirGLO-WT and inhibitor of miR-148b ($p < 0.01$) (Fig. 4E).

In Western blot analysis, treatment with si-HOTAIRs and miR-148b mimic reduced DNMT1 expression and increased PCDH10 expression compared to the control in MKN 28 and MKN 74 cells (Fig. 4F). HOTAIR overexpression increased DNMT1 expression and reduced PCDH10 expression in AGS cell; however, treatment with miR-148b mimic showed the opposite result (Fig. 4F). Finally, we found that DNMT1 was down-regulated after si-HOTAIRs, and it was restored after treatment with miR-148b inhibitor in MKN 28 and MKN 74 cells (Fig. 4G).

DISCUSSION

HOTAIR has been widely studied in various cancers,^{7-9,11,13,14,24-26} and several studies found the key roles of HOTAIR in the gastric carcinogenesis.^{8,14,27} Our results also confirmed that HO-

TAIR was related to the inhibition of apoptosis, proliferation, invasiveness, and metastasis in GC cells, which was in line with our previous study.¹⁴ Moreover, clinicopathologic analysis in GC tissues indicated that high HOTAIR was associated with more advanced TNM stage, which was consistent with previous studies.^{8,10,11,14,28}

PCDH10 was transcriptionally repressed upon HOTAIR expression in breast cancer and GIST.^{7,18} PCDH10 is a potential tumor suppressor gene, and inactivation of PCDH10 by promoter methylation has been studied in various human cancers, including GC.¹⁵⁻¹⁷ Consistent with previous results, the mRNA level of PCDH10 in GC tissues was significantly lower than that in non-tumor tissues in our study.

In this study, we investigated the epigenetic mechanism of HOTAIR in GC, and found that HOTAIR promoted the methylation of PCDH10 by upregulating DNMT1. DNA methylation is mediated by DNMTs, including DNMT1, DNMT3a and DNMT3b, which catalyze the methylation at cytosine-C5 mainly in a CpG dinucleotide context.²⁹ DNMT1 is most widely known to be responsible for the maintenance of DNA methylation.²⁹ Overexpression of DNMT1 has been shown in several cancers, and targeting DNMT1 could be a potential target in the treatment of cancers.²⁹ In a previous study, we reported that lncRNA LUCAT1, which modulates the stability of DNMT1, results in the DNA methylation of tumor suppressor genes.³⁰ DNA methylation in the promoter regions of tumor suppressor genes, which plays an important role in the initiation and progression of tumor, is the most well-defined epigenetic mechanism in GC.³¹⁻³³ Additionally, aberrant methylation of tumor suppressor genes have been associated with clinicopathological characteristics and clinical outcomes in GC,³³ and the promoter methylation appears to be a relatively early event during gastric carcinogenesis.¹⁷ Therefore, our findings may provide a better understanding of early carcinogenesis of GC.

Furthermore, we found that miR-148b could be involved in the reciprocal regulation process of PCDH10 methylation with HOTAIR. To date, researchers have found the role of lncRNAs and miRNAs in gene regulation, and bioinformatic analysis revealed the interaction between lncRNAs and miRNAs in various cancers.^{19,21,24,25,34,35} The role of miR-148a was widely studied by previous researchers, and Song, et al. reported that miR-148b is frequently downregulated in GC and acts as a tumor suppressor.^{20,22} The expression of miR-148b was found to be associated with tumor size in GC patients, and the data also suggested that miR-148b can inhibit cell proliferation in vitro and in vivo.²⁰

In the current study, we found an inverse correlation between HOTAIR and miR-148b by qRT-PCR, and luciferase reporter assay indicated that miR-148b suppresses HOTAIR by binding to HOTAIR in a sequence-specific manner. In Western blot analysis, the expressions of DNMT1 and PCDH10 were regulated by HOTAIR and miR-148b subsequently. These results were similar with the previous findings that HOTAIR may

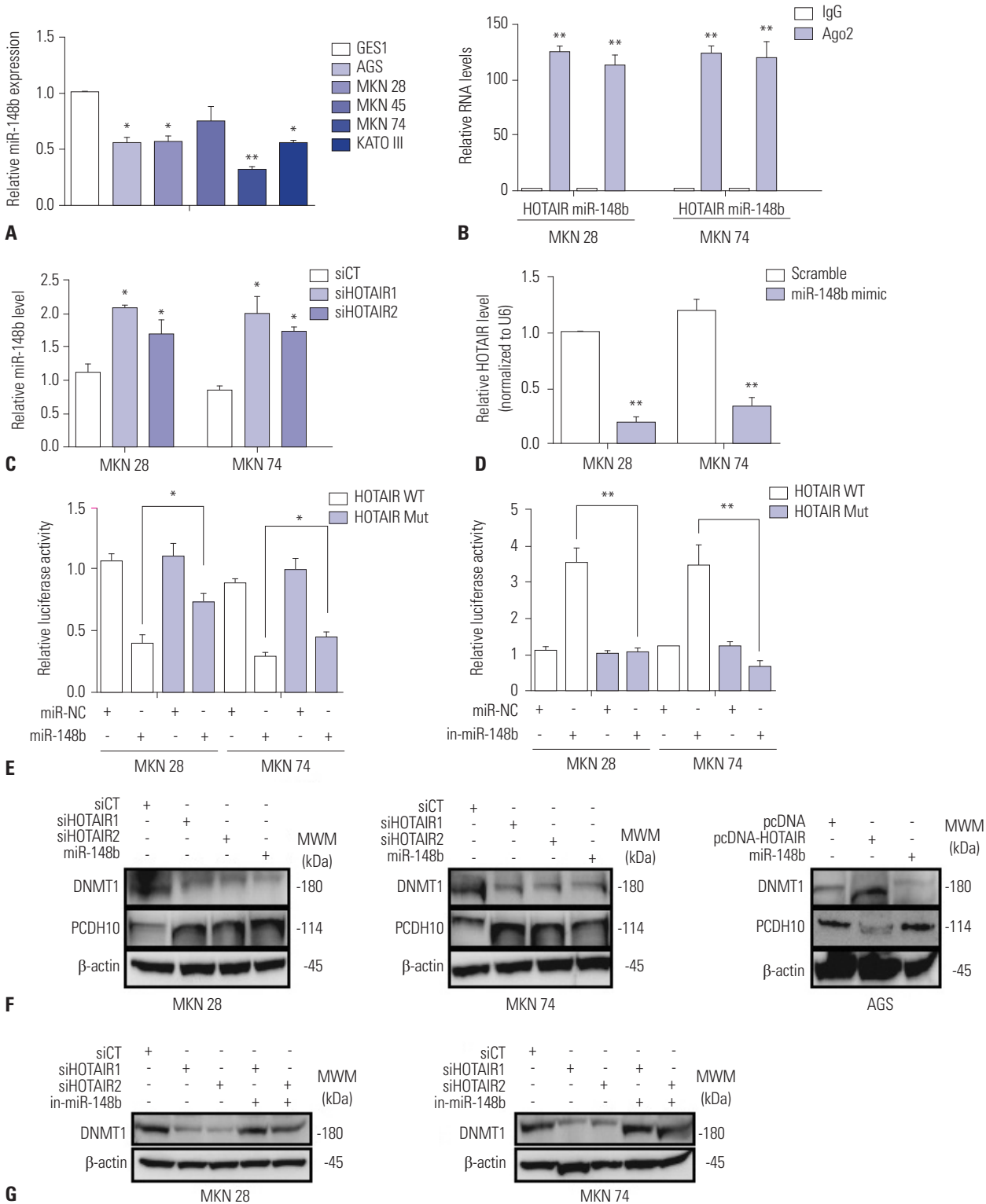


Fig. 4. Reciprocal negative regulation of miR-148b and HOTAIR on PCDH10 expression. (A) The relative miR-148b expression by qRT-PCR in five GC cell lines. (B) RIP with anti-Ago2 was performed in MKN 28 and MKN 74 cells transfected with HOTAIR and miR-148b. HOTAIR and miR-148b expression level were detected using qRT-PCR. (C) The relative miR-148b level after transfection with si-HOTAIRs by qRT-PCR. (D) The relative HOTAIR level after transfection with miR-148b mimic by qRT-PCR. (E) The relative luciferase activity of HOTAIR after treatment with miR-148b mimic/inhibitor in MKN 28 and 74 cells transfected with wild type/mutant type HOTAIR. (F) Western blot analysis of DNMT1 and PCDH10 after treatment with si-HOTAIRs and miR-148b mimic. (G) Western blot analysis of DNMT1 after treatment with si-HOTAIRs and miR-148b inhibitor. Data are presented as the mean±standard deviation of three independent experiments. The asterisk (*) represents a statistically significant difference compared with scrambled control. * $p \leq 0.05$, ** $p \leq 0.01$. HOTAIR, HOX transcript antisense intergenic RNA; PCDH10, protocadherin 10; GC, gastric cancer; RIP, RNA immunoprecipitation.

act as an endogenous sponge of miR-148b, which regulates the expression of DNMT1 in hepatic stellate cells and fibrogenesis in liver.²⁵ Therefore, our results demonstrated the interaction between miRNA and lncRNA in the methylation of well-known tumor suppressor gene.

Finally, as seen in our and other researchers' studies,^{15,18} p53 was important for the transcription of PCDH10, and HOTAIR also reduced the expression of p53 in our study. Since our results showed that the effects of HOTAIR on PCDH10 may be less than that of p53, further studies on how HOTAIR regulates p53 and how p53 regulates PCDH10 are needed to investigate the exact role of PCDH10 in GC.

Our study had some limitations. Firstly, we could not include *in vivo* model to complement our results. Although we collected GC and non-cancer tissues from 49 patients with GC as a means of representative *in vivo* findings to overcome this limitation, caution is needed in the interpretation of our study results. Secondly, quite a few papers have already reported similar HOTAIR action in cancer as demonstrated in this study. Although it might be unique and clear that PCDH10 was the downstream target of HOTAIR in our results, we did not investigate other pathways such as Wnt/beta-catenin signaling pathway.

Taken together, we found a novel epigenetic mechanism of HOTAIR, which was involved in the methylation of PCDH10 by interacting with miR-148b in GC. HOTAIR enhanced the methylation of PCDH10 by upregulating DNMT1 and acted as a ceRNA of miR-148b, which regulated DNMT1 reciprocally. This mechanism may be a potential biomarker and therapeutic target against GC, although it should be further investigated.

ACKNOWLEDGEMENTS

This research was supported by the Basic Science Research Program through National Research Foundation of Korea (NRF) funded by the Ministry of Science and ICT (grant number: NRF-2017R1C1B5076318 and NRF-2020R1A2B5B01002047).

AUTHOR CONTRIBUTIONS

Conceptualization: Sang Kil Lee. **Data curation:** Seung In Seo. **Formal analysis:** Jung-Ho Yoon, Hyo Joo Byun, and Seung In Seo. **Funding acquisition:** Seung In Seo and Sang Kil Lee. **Investigation:** Sang Kil Lee. **Methodology:** Seung In Seo and Jung-Ho Yoon. **Project administration:** Sang Kil Lee. **Resources:** Seung In Seo and Jung-Ho Yoon. **Software:** Seung In Seo and Jung-Ho Yoon. **Supervision:** Sang Kil Lee. **Validation:** Jung-Ho Yoon and Sang Kil Lee. **Visualization:** Jung-Ho Yoon and Hyo Joo Byun. **Writing—original draft:** Seung In Seo, Jung-Ho Yoon, and Sang Kil Lee. **Writing—review & editing:** Seung In Seo and Sang Kil Lee. **Approval of final manuscript:** all authors.

ORCID iDs

Seung In Seo <https://orcid.org/0000-0003-4417-0135>
Jung-Ho Yoon <https://orcid.org/0000-0002-9188-896X>

Hyo Joo Byun <https://orcid.org/0000-0002-7039-9534>
Sang Kil Lee <https://orcid.org/0000-0002-0721-0364>

REFERENCES

- Balakrishnan M, George R, Sharma A, Graham DY. Changing trends in stomach cancer throughout the world. *Curr Gastroenterol Rep* 2017;19:36.
- Torre LA, Bray F, Siegel RL, Ferlay J, Lortet-Tieulent J, Jemal A. Global cancer statistics, 2012. *CA Cancer J Clin* 2015;65:87-108.
- Iyer MK, Niknafs YS, Malik R, Singhal U, Sahu A, Hosono Y, et al. The landscape of long noncoding RNAs in the human transcriptome. *Nat Genet* 2015;47:199-208.
- St Laurent G, Wahlestedt C, Kapranov P. The landscape of long noncoding RNA classification. *Trends Genet* 2015;31:239-51.
- Li T, Mo X, Fu L, Xiao B, Guo J. Molecular mechanisms of long non-coding RNAs on gastric cancer. *Oncotarget* 2016;7:8601-12.
- Geng YJ, Xie SL, Li Q, Ma J, Wang GY. Large intervening non-coding RNA HOTAIR is associated with hepatocellular carcinoma progression. *J Int Med Res* 2011;39:2119-28.
- Gupta RA, Shah N, Wang KC, Kim J, Horlings HM, Wong DJ, et al. Long non-coding RNA HOTAIR reprograms chromatin state to promote cancer metastasis. *Nature* 2010;464:1071-6.
- Hajjari M, Behmanesh M, Sadeghizadeh M, Zeinoddini M. Up-regulation of HOTAIR long non-coding RNA in human gastric adenocarcinoma tissues. *Med Oncol* 2013;30:670.
- Kim K, Jutooru I, Chadalapaka G, Johnson G, Frank J, Burghardt R, et al. HOTAIR is a negative prognostic factor and exhibits pro-oncogenic activity in pancreatic cancer. *Oncogene* 2013;32:1616-25.
- Kogo R, Shimamura T, Mimori K, Kawahara K, Imoto S, Sudo T, et al. Long noncoding RNA HOTAIR regulates polycomb-dependent chromatin modification and is associated with poor prognosis in colorectal cancers. *Cancer Res* 2011;71:6320-6.
- Li X, Wu Z, Mei Q, Li X, Guo M, Fu X, et al. Long non-coding RNA HOTAIR, a driver of malignancy, predicts negative prognosis and exhibits oncogenic activity in oesophageal squamous cell carcinoma. *Br J Cancer* 2013;109:2266-78.
- Xu ZY, Yu QM, Du YA, Yang LT, Dong RZ, Huang L, et al. Knockdown of long non-coding RNA HOTAIR suppresses tumor invasion and reverses epithelial-mesenchymal transition in gastric cancer. *Int J Biol Sci* 2013;9:587-97.
- Yu X, Li Z. Long non-coding RNA HOTAIR: a novel oncogene (Review). *Mol Med Rep* 2015;12:5611-8.
- Lee NK, Lee JH, Park CH, Yu D, Lee YC, Cheong JH, et al. Long non-coding RNA HOTAIR promotes carcinogenesis and invasion of gastric adenocarcinoma. *Biochem Biophys Res Commun* 2014;451:171-8.
- Shi D, Murty VV, Gu W. PCDH10, a novel p53 transcriptional target in regulating cell migration. *Cell Cycle* 2015;14:857-66.
- Ying J, Li H, Seng TJ, Langford C, Srivastava G, Tsao SW, et al. Functional epigenetics identifies a protocadherin PCDH10 as a candidate tumor suppressor for nasopharyngeal, esophageal and multiple other carcinomas with frequent methylation. *Oncogene* 2006;25:1070-80.
- Yu J, Cheng YY, Tao Q, Cheung KF, Lam CN, Geng H, et al. Methylation of protocadherin 10, a novel tumor suppressor, is associated with poor prognosis in patients with gastric cancer. *Gastroenterology* 2009;136:640-51.e1.
- Lee NK, Lee JH, Kim WK, Yun S, Youn YH, Park CH, et al. Promoter methylation of PCDH10 by HOTAIR regulates the progression of gastrointestinal stromal tumors. *Oncotarget* 2016;7:75307-18.
- Dong X, He X, Guan A, Huang W, Jia H, Huang Y, et al. Long non-

- coding RNA Hotaïr promotes gastric cancer progression via miR-217-GPC5 axis. *Life Sci* 2019;217:271-82.
20. Song YX, Yue ZY, Wang ZN, Xu YY, Luo Y, Xu HM, et al. MicroRNA-148b is frequently down-regulated in gastric cancer and acts as a tumor suppressor by inhibiting cell proliferation. *Mol Cancer* 2011;10:1.
 21. Wang G, Li Z, Tian N, Han L, Fu Y, Guo Z, et al. miR-148b-3p inhibits malignant biological behaviors of human glioma cells induced by high HOTAIR expression. *Oncol Lett* 2016;12:879-86.
 22. Xia J, Guo X, Yan J, Deng K. The role of miR-148a in gastric cancer. *J Cancer Res Clin Oncol* 2014;140:1451-6.
 23. Li JH, Liu S, Zhou H, Qu LH, Yang JH. starBase v2.0: decoding miRNA-ceRNA, miRNA-ncRNA and protein-RNA interaction networks from large-scale CLIP-Seq data. *Nucleic Acids Res* 2014;42:D92-7.
 24. Yu F, Chen B, Dong P, Zheng J. HOTAIR epigenetically modulates PTEN expression via MicroRNA-29b: a novel mechanism in regulation of liver fibrosis. *Mol Ther* 2017;25:205-17.
 25. Bian EB, Wang YY, Yang Y, Wu BM, Xu T, Meng XM, et al. Hotaïr facilitates hepatic stellate cells activation and fibrogenesis in the liver. *Biochim Biophys Acta Mol Basis Dis* 2017;1863:674-86.
 26. Abdeahad H, Avan A, Pashirzad M, Khazaei M, Soleimanpour S, Ferns GA, et al. The prognostic potential of long noncoding RNA HOTAIR expression in human digestive system carcinomas: a meta-analysis. *J Cell Physiol* 2019;234:10926-33.
 27. Xu Z, Chen H, Yang B, Liu X, Zhou X, Kong H. The association of HOTAIR with the diagnosis and prognosis of gastric cancer and its effect on the proliferation of gastric cancer cells. *Can J Gastroenterol Hepatol* 2019;2019:3076345.
 28. Liu FT, Qiu C, Luo HL, Zhang Y, Xia GF, Hao TF, et al. The association of HOTAIR expression with clinicopathological features and prognosis in gastric cancer patients. *Panminerva Med* 2016;58:167-74.
 29. Xiang S, Zou P, Tang Q, Zheng F, Wu J, Chen Z, et al. HOTAIR-mediated reciprocal regulation of EZH2 and DNMT1 contribute to polyphyllin I-inhibited growth of castration-resistant prostate cancer cells in vitro and in vivo. *Biochim Biophys Acta Gen Subj* 2018;1862:589-99.
 30. Yoon JH, You BH, Park CH, Kim YJ, Nam JW, Lee SK. The long non-coding RNA LUCAT1 promotes tumorigenesis by controlling ubiquitination and stability of DNA methyltransferase 1 in esophageal squamous cell carcinoma. *Cancer Lett* 2018;417:47-57.
 31. Maeda M, Moro H, Ushijima T. Mechanisms for the induction of gastric cancer by *Helicobacter pylori* infection: aberrant DNA methylation pathway. *Gastric Cancer* 2017;20:8-15.
 32. Tan P, Yeoh KG. Genetics and molecular pathogenesis of gastric adenocarcinoma. *Gastroenterology* 2015;149:1153-62.e3.
 33. Qu Y, Dang S, Hou P. Gene methylation in gastric cancer. *Clin Chim Acta* 2013;424:53-65.
 34. Sa L, Li Y, Zhao L, Liu Y, Wang P, Liu L, et al. The role of HOTAIR/miR-148b-3p/USF1 on regulating the permeability of BTB. *Front Mol Neurosci* 2017;10:194.
 35. Zhang JG, Shi Y, Hong DF, Song M, Huang D, Wang CY, et al. MiR-148b suppresses cell proliferation and invasion in hepatocellular carcinoma by targeting WNT1/ β -catenin pathway. *Sci Rep* 2015;5:8087.